

Award Number: W81XWH-10-1-0058

TITLE: Augmentation of Breast Cancer Growth and Metastasis by Chronic Stressor Exposure

PRINCIPAL INVESTIGATOR: Mercedes Szpunar

CONTRACTING ORGANIZATION: University of Rochester  
Rochester, NY 14611

REPORT DATE: July 2012

TYPE OF REPORT: Annual Summary

PREPARED FOR: U.S. Army Medical Research and Materiel Command  
Fort Detrick, Maryland 21702-5012

DISTRIBUTION STATEMENT: Approved for public release; distribution unlimited

The views, opinions and/or findings contained in this report are those of the author(s) and should not be construed as an official Department of the Army position, policy or decision unless so designated by other documentation.

<b>REPORT DOCUMENTATION PAGE</b>				<i>Form Approved</i> <b>OMB No. 0704-0188</b>	
<small>Public reporting burden for this collection of information is estimated to average 1 hour per response, including the time for reviewing instructions, searching existing data sources, gathering and maintaining the data needed, and completing and reviewing this collection of information. Send comments regarding this burden estimate or any other aspect of this collection of information, including suggestions for reducing this burden to Department of Defense, Washington Headquarters Services, Directorate for Information Operations and Reports (0704-0188), 1215 Jefferson Davis Highway, Suite 1204, Arlington, VA 22202-4302. Respondents should be aware that notwithstanding any other provision of law, no person shall be subject to any penalty for failing to comply with a collection of information if it does not display a currently valid OMB control number. <b>PLEASE DO NOT RETURN YOUR FORM TO THE ABOVE ADDRESS.</b></small>					
<b>1. REPORT DATE (DD-MM-YYYY)</b> 01-07-2012		<b>2. REPORT TYPE</b> Annual Summary		<b>3. DATES COVERED (From - To)</b> 1 JUL 2011 - 30 JUN 2012	
<b>4. TITLE AND SUBTITLE</b> Augmentation of Breast Cancer Growth and Metastasis by Chronic Stressor Exposure				<b>5a. CONTRACT NUMBER</b>	
				<b>5b. GRANT NUMBER</b> W81XWH-10-1-0058	
				<b>5c. PROGRAM ELEMENT NUMBER</b>	
<b>6. AUTHOR(S)</b> Mercedes Szpunar  E-Mail:				<b>5d. PROJECT NUMBER</b>	
				<b>5e. TASK NUMBER</b>	
				<b>5f. WORK UNIT NUMBER</b>	
<b>7. PERFORMING ORGANIZATION NAME(S) AND ADDRESS(ES)</b> University of Rochester Rochester, NY 14611				<b>8. PERFORMING ORGANIZATION REPORT NUMBER</b>	
<b>9. SPONSORING / MONITORING AGENCY NAME(S) AND ADDRESS(ES)</b> U.S. Army Medical Research and Materiel Command Fort Detrick, Maryland 21702-5012				<b>10. SPONSOR/MONITOR'S ACRONYM(S)</b>	
				<b>11. SPONSOR/MONITOR'S REPORT NUMBER(S)</b>	
<b>12. DISTRIBUTION / AVAILABILITY STATEMENT</b> Approved for Public Release; Distribution Unlimited					
<b>13. SUPPLEMENTARY NOTES</b>					
<b>14. ABSTRACT</b> Abstract on next page.					
<b>15. SUBJECT TERMS</b> breast cancer, sympathetic nervous system, norepinephrine, angiogenesis, VEGF, SHG					
<b>16. SECURITY CLASSIFICATION OF:</b>			<b>17. LIMITATION OF ABSTRACT</b>	<b>18. NUMBER OF PAGES</b>	<b>19a. NAME OF RESPONSIBLE PERSON</b>
<b>a. REPORT</b> U	<b>b. ABSTRACT</b> U	<b>c. THIS PAGE</b> U			<b>19b. TELEPHONE NUMBER (include area code)</b>
			UU	26	

#### 14. ABSTRACT

Cancer patients often experience chronic emotional stress with diagnosis and successive treatment. Psychosocial stressors can activate the sympathetic nervous system (SNS) to release the catecholamine norepinephrine (NE), which can stimulate alpha- and beta-adrenergic receptors (alpha- and beta-AR). AR stimulation by NE or other agonists has been shown to influence tumor growth *in vitro* and *in vivo* through induction of angiogenesis and/or metastasis. Our laboratory studies tumor collagen structure through an optical technique called second harmonic generation (SHG). Changes in collagen structure, as manifested by changes in SHG, can alter tumor growth and metastasis. Our objective is to delineate the role of NE and AR stimulation in breast cancer growth and metastasis in the 4T1 murine tumor model. To mimic SNS activation, female BALB/c mice were implanted with slow-release pellets containing desipramine (DMI) – a tricyclic antidepressant that prevents NE reuptake from noradrenergic synapses. DMI treatment increased 4T1 primary tumor growth, but the DMI-induced growth was not associated with altered tumor vasculature or metastasis. However, tumor sections from DMI-implanted mice exhibited altered SHG intensity, demonstrating changes in tumor collagen structure. Tumor growth and metastasis were increased in mice treated with dexmedetomidine (DEX), a highly selective  $\alpha 2$ -AR agonist, but not isoproterenol ( $\beta$ -AR agonist) or phenylephrine ( $\alpha 1$ -AR agonist). The DEX-induced alterations in tumor progression were also associated with alterations in collagen structure as measured by SHG. These results reveal an undescribed role for  $\alpha 2$ -AR in tumor progression, and suggest a novel pathway by which elevated NE may promote tumor progression through the extracellular matrix. *By understanding the impact of SNS activation on breast cancer pathogenesis, we could identify pharmacological means that block sympathetic activation effects that can be of therapeutic benefit for breast cancer patients.*

#### 15. SUBJECT TERMS

## **Table of Contents**

<b>Introduction.....</b>	<b>5</b>
<b>Body.....</b>	<b>5</b>
<b>Key Research Accomplishments.....</b>	<b>15</b>
<b>Reportable Outcomes.....</b>	<b>15</b>
<b>Conclusion.....</b>	<b>17</b>
<b>References.....</b>	<b>18</b>
<b>Appendix.....</b>	<b>20</b>

## INTRODUCTION

Cancer patients often experience chronic emotional stress and/or other negative psychological factors, such as depression or lack of social support, with diagnosis and successive treatment. A recent clinical trial showed that reducing stress decreased cancer recurrence and related-death in breast cancer survivors [1]. Using animal models of cancer, reports examining the influence of stress, in the form of sympathetic nervous system (SNS) activation, on tumor progression have primarily focused on tumor cell lines that express  $\beta$ -adrenergic receptors ( $\beta$ -AR). In a  $\beta$ -AR-expressing ovarian tumor model, SNS activation in the form of direct  $\beta$ -AR stimulation or restraint stress exposure increased primary tumor growth, by means of increased tumor angiogenesis and elevated vascular endothelial growth factor (VEGF) [2]. Sloan and colleagues [3] demonstrated in a murine breast tumor model that the stress-induced increase in metastasis was mediated through increased tumor-associated macrophages (TAMs) that express  $\beta$ -AR. TAMs are known to produce a variety of protumorigenic factors to further tumor progression, such as prometastatic factors, proteases, and proinflammatory cytokines, e.g., interleukins (IL), matrix metalloproteinases (MMPs), and tumor necrosis factor- $\alpha$  (TNF- $\alpha$ ) to name a few [4,5]. The stress effects in both described in vivo experiments were inhibited by  $\beta$ -antagonists, demonstrating a  $\beta$ -AR-mediated mechanism. Breast cancer cell lines and primary human breast tumors are heterogeneous in  $\beta$ -AR expression and signaling capacity [6-9], ranging from no detectable  $\beta$ -AR to very high levels. Of note, the stress response can activate both  $\alpha$ -adrenergic receptors ( $\alpha$ -AR) and  $\beta$ -AR. Although less is known about tumor cell  $\alpha$ -AR expression,  $\alpha$ -AR have been detected in breast cancer cell lines [10] and in primary human breast cancers, and high expression of AR has been linked to poor prognosis [9]. Host stromal cells within a mammary tumor, such as immune cells, mammary endothelial cells, and fibroblasts, are also known to express  $\alpha$ - and  $\beta$ -AR [11-13]. Hence, *we hypothesized that stress-induced norepinephrine (NE) release stimulates breast tumor progression through AR stimulation*. Given the molecular heterogeneity of AR expression, it is important to understand the range of mechanisms that may contribute to stress-induced alterations in tumor pathogenesis.

## BODY

### **Task 1: Continue formal and informal education in oncology.**

#### 1a. Formal education in oncology. (18 months)

I gave a poster presentation at the American Association for Cancer Research (AACR) on Tumor Microenvironment in November 2011 in Orlando, FL. In addition, I gave an oral presentation at the Gordon Research Seminar on Mammary Gland Biology and a poster at the Gordon Research Conference on Mammary Gland Biology in June 2012 in Barga, Italy.

#### 1b. Informal education in oncology. (ongoing)

I have continued to participate in weekly lab meetings, where members of the lab present their research or papers about tumor biology. I also attend lectures relevant to my research, including talks hosted by the Breast Cancer Research Group (part of the University of Rochester's James P. Wilmot Cancer Center).

1c. Laboratory training. (ongoing)

I have continued laboratory training and writing pertinent to my thesis project. In the spring of 2012, I wrote my dissertation titled, “Evidence for Sympathetic Nervous System Regulation of Breast Cancer Progression.” I defended my thesis in June 2012, hence the request to terminate my DoD BRCP fellowship a year early (June 2012 instead of June 2013) since I will be returning to medical school during the last year of the fellowship allotment.

1d. Clinical training. (ongoing)

I am re-entering the University of Rochester School of Medicine in July 2012 to complete my 3<sup>rd</sup> & 4<sup>th</sup> years of medical school.

**Task 2: Determine if chronic stressor exposure stimulates breast tumor growth and metastasis, and if the stress effect can be inhibited by  $\beta$ -adrenergic receptor ( $\beta$ -AR) blockade.**

(Months 0-24)

Task 2a: Measure the catecholamine response to social isolation. (2-5 months)

This task was described in depth in the last report (submitted August 2011).

Task 2b: Determine if chronic stressor exposure alters orthotopic tumor growth and metastasis in mice. (6-12 months)

In the last report, we explained how we revised our social isolation stressor model using the human MB-231 breast cancer cell line in two ways: 1) we utilized the treatment desipramine (DMI), a NE-reuptake inhibitor used to treat patients suffering from depression, to elevate NE as a pharmacologic “stressor” exposure; and 2) we altered our *in vivo* tumor model to 4T1, a murine mammary adenocarcinoma cell line, which is grown in immunocompetent BALB/c mice and quickly metastasizes to the lung from the primary tumor when injected into the mammary fat pad. We had previously determined that 4T1 cells express no detectable  $\beta$ -AR and do not respond to  $\beta$ -AR agonists with elevated cAMP (data not shown), and hence, we viewed 4T1 as a good model for examining NE effects on the tumor stromal cells in the absence of direct involvement of  $\beta$ -AR-expressing tumor cells. In that report, we showed that 21-day release 10 mg DMI pellets, which chronically delivered about 0.5 mg DMI per day, significantly augmented 4T1 primary tumor growth and increased NE in the spleen. However, it did not alter lung metastasis, and the DMI-treated tumors produced a significant decrease in VEGF, an unexpected effect considering the increased primary tumor growth.

**DMI Decreases 4T1 Tumor VEGF but Does Not Alter Blood Vessel Density**

To determine if there was a change in tumor blood vessel density due to decreased VEGF, sections from 4T1 tumors were stained by immunocytochemistry (ICC) for CD31<sup>+</sup> endothelial cells. Using multiphoton laser scanning microscopy (MPLSM), five random images of one tumor section per tumor were imaged by a blinded observer at 810 nm excitation wavelength and at the same power (100 mW) and detector settings. To detect immunofluorescence, fluorophore emission was collected using bandpass filters 635/30 for the Alexa-Fluor 594 secondary

antibody. Figure 1A shows a representative image of the tumor blood vessels imaged using MPLSM. To quantify immunofluorescence, the percentage of pixels above threshold was calculated, and all images were analyzed using custom-written algorithms in ImageJ (NIH Freeware). However, there was no difference in blood vessel density between DMI-treated and placebo tumors (Figure 1B) despite the decrease in tumor VEGF in the treated tumors.

A.

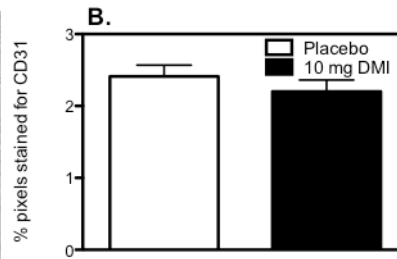
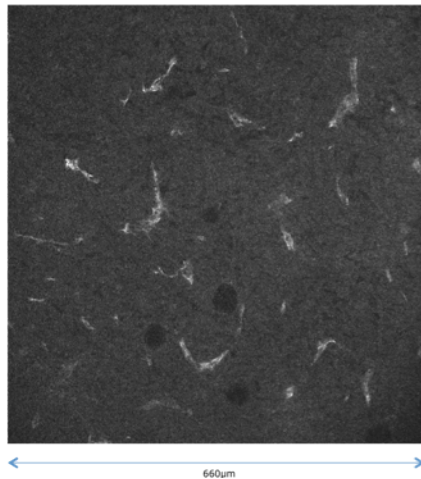


Figure 1. A) Representative ICC fluorescent staining of CD31<sup>+</sup> blood vessels in a 4T1 tumor as imaged by MPLSM. B) Percentage of CD31<sup>+</sup> pixels above threshold from the 4T1 tumors. Results are expressed as mean  $\pm$  SEM, n=9 placebo & DMI.

### DMI Alters 4T1 Tumor TNF- $\alpha$ but Not Macrophage Density

To further investigate mechanism(s) underlying DMI-induced tumor growth, we measured several proangiogenic and prometastatic factors. We found no difference in tumor IL-6, IL-1 $\beta$ , or MMP-9 concentrations (Figure 2A-C) at day 14 after tumor cell injection, when the experiment was ended because of increased tumor growth (see previous report). However, TNF- $\alpha$  was doubled in the DMI-treated tumors (Figure 2D; student's t-test, p=0.026).

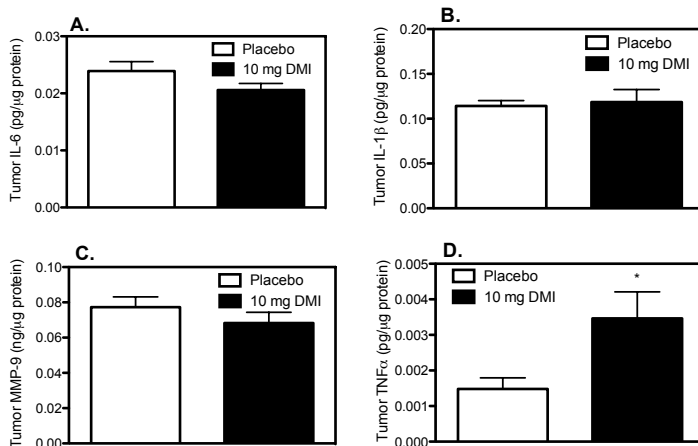


Figure 2. IL-6 (A), IL-1 $\beta$  (B), MMP-9 (C), and TNF- $\alpha$  (D) production by tumors harvested 14 days after 4T1 tumor cell injection. Results are expressed as mean  $\pm$  SEM, n=9 placebo & DMI. \*p<0.05 versus placebo by student's t-test.

Since TNF- $\alpha$  is produced by macrophages and enhances tumor progression [5], we asked if increased TNF- $\alpha$  production was associated with increased number of macrophages. 4T1 tumor sections were stained by ICC for F4/80<sup>+</sup> macrophages, imaged with MPLSM, and quantified as

described for CD31<sup>+</sup> endothelial cells. Figure 3A is a representative image of F4/80<sup>+</sup> stained macrophages from a 4T1 tumor as imaged by MPLSM, and image analysis of the percentage of pixels above threshold revealed no difference in macrophage density between DMI-treated and placebo tumors (Figure 3B).

A.

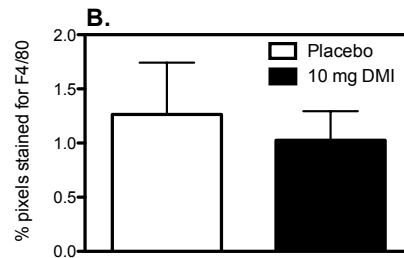
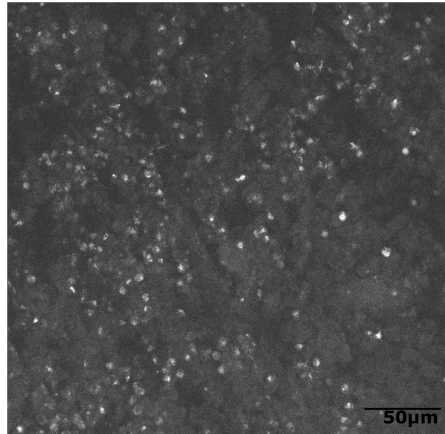
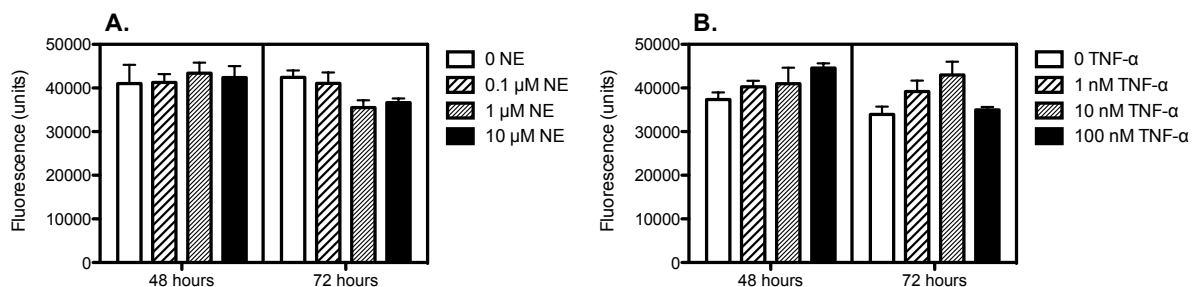


Figure 3. A) Representative ICC fluorescent staining for F4/80<sup>+</sup> macrophages as imaged by MPLSM. B) Percentage of F4/80<sup>+</sup> pixels above threshold from the 4T1 tumors (B). Results are expressed as mean  $\pm$  SEM, n=9 placebo & DMI.

### In vitro, NE and TNF- $\alpha$ Do Not Alter 4T1 Proliferation, and NE Does Not Alter 4T1 VEGF Production

The DMI results presented in the previous report and here imply that a DMI-induced increase in NE availability caused alterations in 4T1 tumor pathogenesis. It is our contention that if such changes occur in the tumor, it is unlikely that the effects of DMI are mediated through direct interaction of NE with 4T1 tumor cells. To further confirm that NE is unlikely to act directly on 4T1 tumor cells, we tested 4T1 proliferation and VEGF production in vitro. Varying concentrations of NE were unable to alter 4T1 proliferation (Figure 4A) and VEGF production (Figure 4C). These results are consistent with our previous 4T1 results demonstrating the lack of  $\beta$ -AR expression and  $\beta$ -AR-induced cAMP production (data not shown). Furthermore, since DMI-treated tumors increased TNF- $\alpha$ , we tested if TNF- $\alpha$  was capable of altering 4T1 proliferation in vitro, but it did not (Figure 4B). Under our low-serum culture conditions, 4T1 production of TNF- $\alpha$  is not detectable. These results suggest that it is unlikely that NE can directly stimulate 4T1 cells in isolation to alter tumor growth.



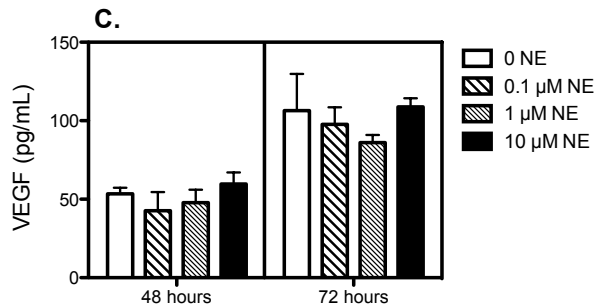


Figure 4. 4T1 cells were incubated in vitro with 0-10  $\mu$ M NE (A) or 0-100 nM TNF- $\alpha$  (B), and proliferation was determined after 48 and 72 hours in culture. C) Mouse VEGF production was measured in 4T1 cell culture supernatant removed after 48 and 72 hours in culture with 0-10  $\mu$ M NE. Results are expressed as mean  $\pm$  SEM, n=3.

### $\alpha$ 2-AR Stimulation, but Not $\alpha$ 1-AR and $\beta$ -AR Stimulation, Alters 4T1 Tumor Growth and Metastasis

In the next experiment, we sought to determine the AR mediating DMI-induced changes in tumor growth. NE can stimulate both  $\alpha$ - and  $\beta$ -AR, but in the 4T1 tumor model,  $\beta$ -AR are only present on the tumor stromal cells since they are not present or signaling through 4T1 tumor cells. We employed daily intraperitoneal injections to mimic what others had found effective in the context of increased tumor pathogenesis following  $\beta$ -AR stimulation with isoproterenol (ISO) [2,3]. We performed pilot experiments to establish doses of the following AR agonists: ISO, a nonselective  $\beta$ -AR agonist; phenylephrine (PE), an  $\alpha$ 1-AR agonist; and dexmedetomidine (DEX), a highly selective  $\alpha$ 2-AR agonist. We tested a range of doses based on the literature to elicit physiological alterations and to ensure that we did not elicit overt toxicity. At the dose of 10 mg/kg ISO (3 mice), two of the mice died by day three post tumor injection. At 5 mg/kg ISO (3 mice), all mice displayed excitatory behavior when handled, such as increased activity and jumpiness, but no mice died, so this dose was used as the experimental dose. PE was administered at doses of 5 mg/kg and 10 mg/kg. The mice also exhibited some excitatory behavior after drug administration, but all mice survived so 10 mg/kg was chosen as the experimental dose. Both ISO and PE elicited a loss in body weight followed by recovery, similar to that of DMI (data not shown). DEX is often used as an anesthetic, which was not our goal with the treatment. Initially, we administered DEX at doses ranging from 10 to 200  $\mu$ g/kg to one mouse each. Mice receiving 25 to 100  $\mu$ g/kg all showed slowed behavior, and the mouse receiving 200  $\mu$ g/kg was completely anesthetized, but all mice recovered within an hour of treatment. We chose 10  $\mu$ g/kg as a dose of DEX that does not elicit sedative behavioral changes. Agonists were delivered in sterile saline, and initiated two days prior to 4T1 injection and continued once daily throughout the duration of the experiment, similar to our protocol of chronic DMI treatment in which the slow-release pellets were implanted two days prior to tumor cell injection.

In mice treated with ISO or PE, there were no differences in tumor volume (Figure 5A, C) or weight (Figure 5B, D) compared to saline. However, the mice treated with DEX developed significantly larger tumors by day 19 (Figure 5E; repeated measures two-way ANOVA, main effect of DEX treatment,  $p=0.10$ ; DEX x time interaction,  $p=0.002$ ; time,  $p<0.0001$ ; by

Bonferonni post-hoc analysis,  $p < 0.01$  on day 19). There was a trend toward increased tumor weight at sacrifice on day 19 in the DEX-treated mice (Figure 5F; student's t-test,  $p = 0.095$ ).

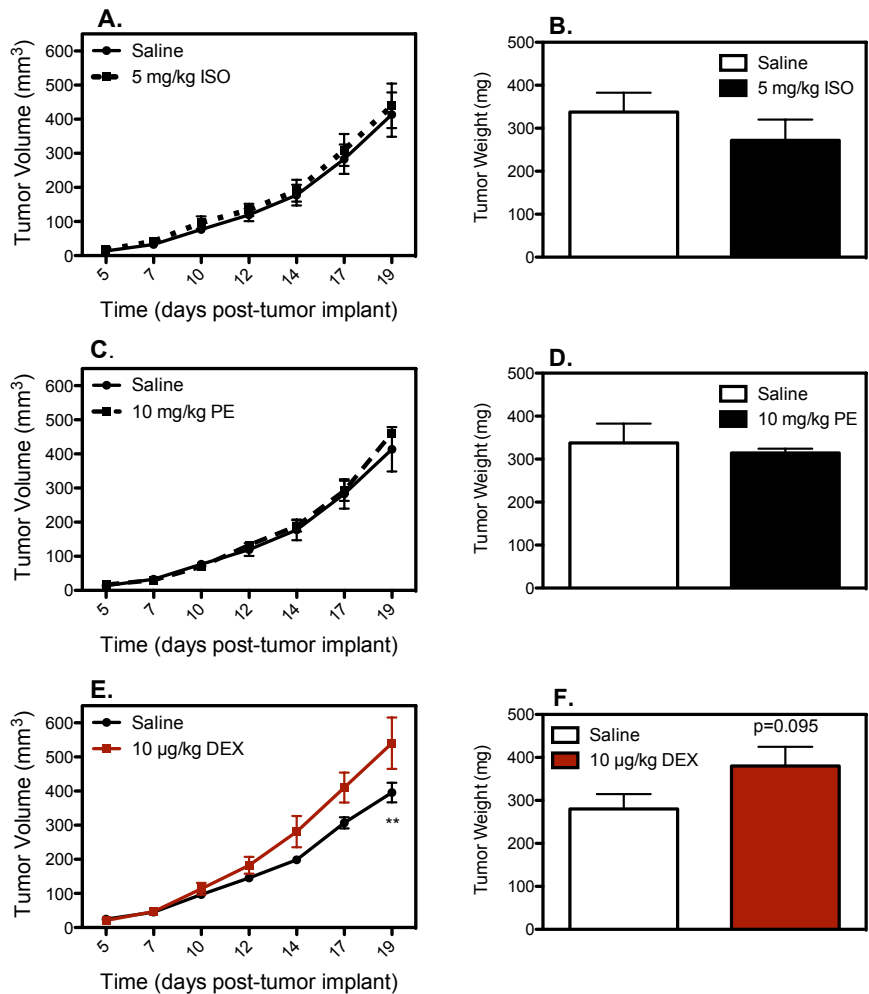
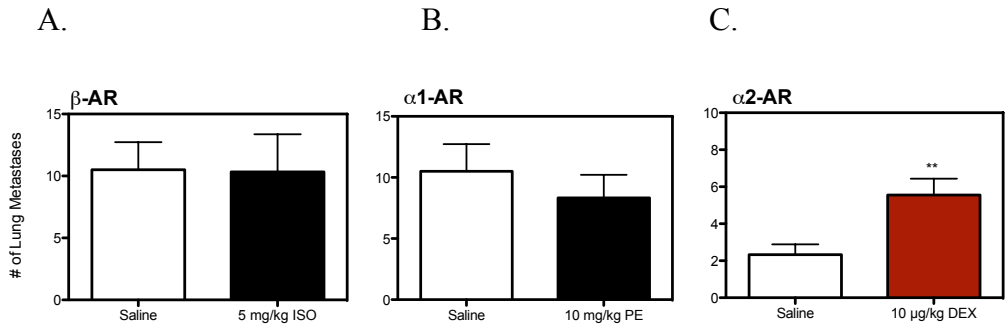


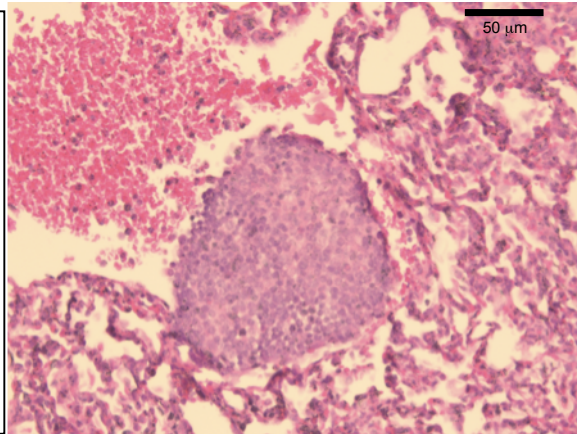
Figure 5. Beginning 2 days prior to 4T1 cell injection, mice were injected daily with saline or 5 mg/kg ISO (A,B), 10 mg/kg PE (C,D), or 10 µg/kg DEX (E,F). Tumor volume over time and weight at sacrifice 19 days after 4T1 injection. Results are expressed as mean  $\pm$  SEM,  $n = 6$  saline & ISO or PE,  $n = 9$  saline & DEX. \*\* $p < 0.01$  versus saline by Bonferonni post-hoc analysis.

At termination of the experiment, lungs were fixed in formalin, paraffin-embedded, and sliced before staining by standard hematoxylin and eosin (H & E) techniques. Metastatic foci were visualized using a 4X objective lens and counted in each tissue section by a blinded observer. Metastases were not altered in ISO- or PE-treated mice (Figure 6A, B), but DEX significantly increased the number of metastasis to the lung (Figure 6C; student's t-test,  $p = 0.007$ ).



D.

Figure 6. Beginning 2 days prior to 4T1 cell injection, mice were injected daily with saline or 5 mg/kg ISO (A), 10 mg/kg PE (B), or 10  $\mu$ g/kg DEX (C). D) Representative image of a 4T1 lung metastasis from a DEX-treated mouse. Results are expressed as mean  $\pm$  SEM, n=6 saline & ISO or PE, n=9 saline & DEX. \*\*p<0.01 versus saline by student's t-test.



### $\alpha$ 2-AR Stimulation Alters Macrophage Density But Not Tumor Cytokines

The DEX-induced increase in tumor growth was not associated with significant alterations in tumor VEGF, IL-6, or TNF- $\alpha$  (Figure 7A-C). Immunocytochemical analysis of tumor F4/80<sup>+</sup> macrophages revealed a borderline significant increase in macrophage density in the DEX-treated group (Figure 7D; student's t-test, p=0.056). Therefore,  $\alpha$ 2-AR-induced increase in tumor growth and metastasis is associated with increased numbers of TAMs.

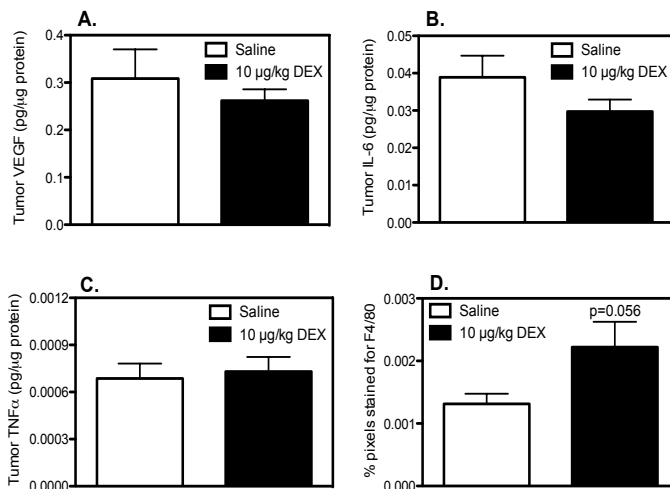


Figure 7. Beginning 2 days prior to 4T1 cell injection, mice were injected daily with saline or 10  $\mu$ g/kg DEX, and tumors were harvested 19 days after 4T1 tumor cell injection. VEGF (A), IL-6 (B), and TNF- $\alpha$  (C) production and percentage of F4/80<sup>+</sup> pixels above threshold as imaged by MPLSM (D) from the 4T1 tumors. Results are expressed as mean  $\pm$  SEM, n=9 saline & DEX.

2c: Determine if chronic stress-induced alterations in breast cancer growth *in vivo* can be blocked by a clinically available  $\beta$ -AR antagonist. (6-12 months)

Due to the inability to show a consistent elevation in stress-induced tumor growth in our previous report, we did not test  $\beta$ -AR blockade in the context of stress. Instead, we utilized specific agonists for  $\alpha$ 1-AR,  $\alpha$ 2-AR, and  $\beta$ -AR to delineate the receptor responsible for changes in 4T1 tumor growth and metastasis (see Task 2b). Interesting,  $\beta$ -AR to not appear to be the sole

AR responsible for these changes. Rather,  $\alpha 2$ -AR are capable of inducing increased primary tumor growth in the 4T1 tumor model.

**Task 3: Determine if breast cancer metastasis to the brain increases with chronic stressor exposure and, further, if it can be inhibited by  $\beta$ -AR blockade.**

(Months 8-20)

We have no progress to report on this task since we altered our tumor model to one that does not metastasize to the brain. However, we did report on alterations with 4T1 metastasis to the lung with AR stimulation (see Figure 6). We found  $\alpha 2$ -AR, not  $\beta$ -AR, to be the critical AR in the 4T1 tumor model.

**Task 4: Determine if chronic stressor exposure alters the ordering of collagen in tumors as quantified with second harmonic generation (SHG).**

(Months 20-32)

The structure of the collagenous extracellular matrix is believed to play a pivotal role in the early steps of tumor cell migration and metastasis [14]. The arrangement of collagen fibers is uniquely visible under MPLSM with an optical process called second harmonic generation (SHG) [15]. SHG is an endogenous optical signal produced when two excitation photons combine to produce one emission photon, “catalyzed” by an anisotropic structure, such as ordered collagen triple helices [16]. In murine breast tumor models, tumor cells move towards blood vessels along fibers that are visible via SHG [17]. Tumor cells moving along SHG-producing collagen fibers move more efficiently through tissue than those cells moving independently of SHG-producing fibers [18], and the extent of SHG-associated tumor cell motility is correlated with metastatic ability of the tumor model [19]. Furthermore, the tumor-host interface of murine breast tumor models is characterized by SHG-producing collagen fibers that are associated with tumor cells that can invade the surrounding tissue [20]. Finally, in human breast cancer samples, the presence of these SHG-producing fibers is a prognostic indicator of disease-free survival, independent of grade, size, and receptor status [21].

The same 4T1 tumor sections that were processed for ICC in the 10 mg DMI and the 10  $\mu$ g/kg DEX experiments (described in Task 2b) were used for SHG analysis. SHG signal propagated back from the tissue towards the excitation objective lens was separated from the fluorophore-generated fluorescence by a 475 nm long-pass dichroic (Semrock) and detected with a bandpass 405/30 emission filter. All images were analyzed using custom-written algorithms in ImageJ (NIH Freeware). Figure 8A is a representative image of SHG-producing collagen in a 4T1 tumor. Analysis of the percentage of SHG pixels above threshold revealed no difference in the DMI-treated tumors (Figure 8B), but the intensity of those SHG pixels was increased (Figure 8C; student’s t-test,  $p=0.035$ ). Alternatively, the DEX-treated tumors did not show a difference in the intensity of SHG pixels above threshold (Figure 8E), but they did have increased percentage of pixels above threshold (Figure 8D; student’s t-test,  $p=0.038$ ).

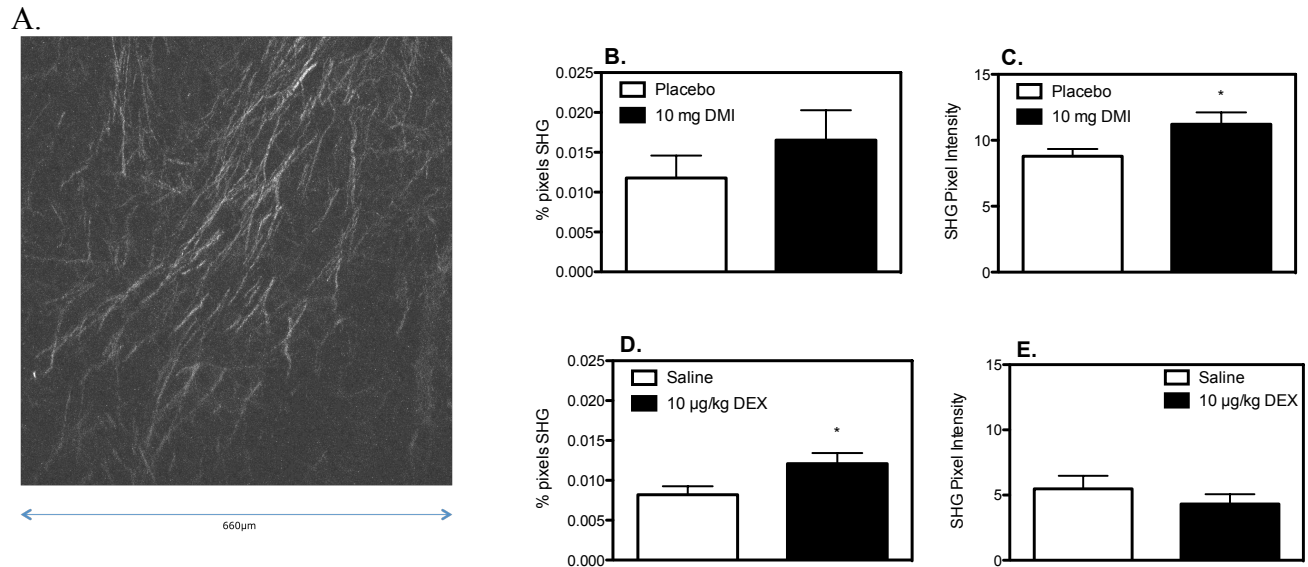


Figure 8. Following treatment with pellets (placebo or 10 mg DMI) or daily injections (saline or 10 μg/kg DEX), tumors were harvested 14 or 19 days after 4T1 tumor cell injection. A) Representative image of SHG as imaged by MPLSM. Percentage of SHG pixels above threshold (B) and SHG pixel intensity (C) from 4T1 tumors in 10 mg DMI experiment. Percentage of SHG pixels above threshold (D) and SHG pixel intensity (E) from 4T1 tumors in 10 μg/kg DEX experiment. Results are expressed as mean ± SEM, n=9 placebo & DMI, n=9 saline & DEX. \*p<0.05 versus placebo or saline by student's t-test.

These alterations in SHG indicate differences in collagen structure within tumors treated with either DMI or DEX that correlate with augmentation of primary tumor growth (for DMI) or with tumor growth and metastasis (for DEX). An interpretation of the DMI-treated tumor SHG result is that there is no increase in production of that class of collagen with the structure necessary to generate detectable SHG (hence no increase in percentage of pixels above threshold) but that the microstructure of that class of collagen is itself altered (hence leading to an increase in intensity of those pixels); we will call this an alteration in “SHG<sup>+</sup> fiber microstructure.” On the other hand, the DEX-treated tumors showed an increase in the percentage of pixels above threshold without an increase in the brightness of those pixels above threshold. An interpretation of this SHG result is that there is more production of that class of collagen with the structure necessary to generate detectable SHG (hence an increase in the percentage of pixels above threshold), but no significant change in the microstructure of that class (hence no increase in intensity of those pixels); we will call this an increase in “SHG<sup>+</sup> fiber content.” One interpretation of the incongruent SHG results between DMI and DEX is that DEX stimulation of α<sub>2</sub>-AR leads to a series of steps within the tumor culminating in an alteration in SHG<sup>+</sup> fiber content (Figure 9).

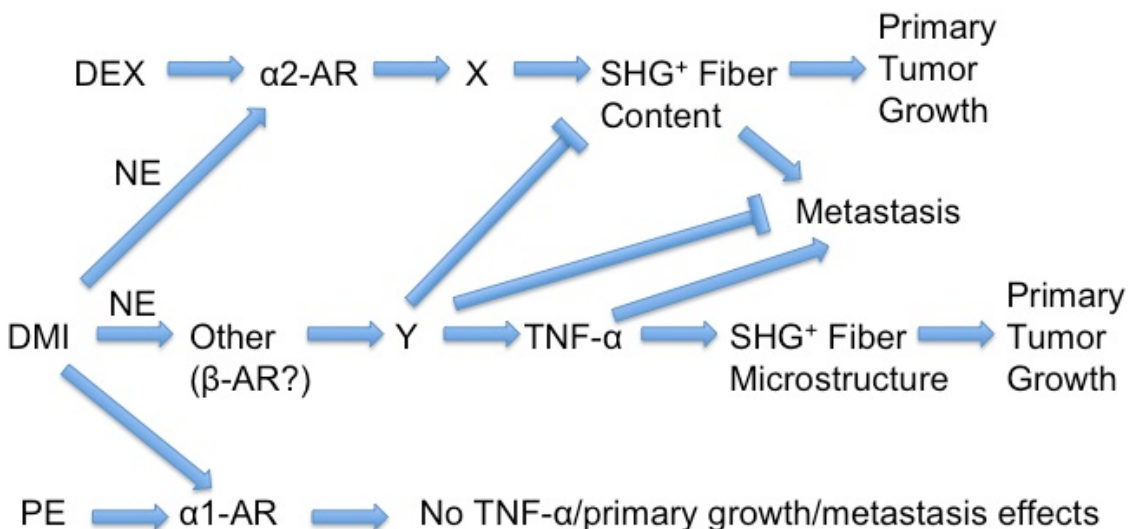


Figure 9. Proposed mechanisms of 4T1 tumor progression after AR stimulation.

This increase provides a progrowth, prometastatic microenvironment for the tumor cells. However, NE stimulates  $\alpha 2$ -AR but also “other” receptors (see below), which themselves produce a series of actions. One of those actions is a blockade of the increase in SHG<sup>+</sup> fiber content and hence a blockade of the subsequent progrowth and prometastatic effects as seen with DEX treatment. However, another consequence is an alteration in SHG<sup>+</sup> fiber microstructure, which apparently has progrowth but not prometastatic effects. We can add some detail to this proposed model when we observe that, interestingly, DMI treatment increased TNF- $\alpha$  in the tumor, while DEX did not. In another research project in our laboratory, E0771 murine mammary adenocarcinoma grown in TNF- $\alpha$ <sup>-/-</sup> mice had a significantly lower intensity of SHG pixels above threshold without a significant change in percentage of pixels above threshold (data not shown), which is consistent with the observed SHG and TNF- $\alpha$  effects after DMI treatment. This effect suggests that the same processes downstream of NE that inhibit a change in SHG<sup>+</sup> fiber content also directly inhibit tumor metastasis, perhaps through direct effects on tumor cell motility, and that this inhibition is induced by DMI treatment upstream of TNF- $\alpha$  expression.

The identification of the “other” receptors stimulated by DMI to induce its effects is rendered difficult by our observation that PE ( $\alpha 1$ -AR specific) and ISO ( $\beta$ -AR specific) had no significant effects on tumor growth or metastasis. However, in the literature, metastatic effects were observed after ISO treatment at the dose of 10 mg/kg [3]. Our ISO experiments were limited to the lower dose of 5 mg/kg due to excessive animal fatalities at the 10 mg/kg dose, which were not reportedly observed by others [2,3]. Furthermore, we have yet to examine the impact of ISO on tumor SHG and changes in other tumor cytokines that may provide evidence for  $\beta$ -AR-mediated effects on 4T1 tumor pathogenesis. Consequently, we conclude that the “other” receptor by which DMI-induced effects through NE could be  $\beta$ -AR, and one interpretation of the results from these experiments is given by Figure 9. In the future, we intend to readdress the role of  $\beta$ -AR in the 4T1 DMI model.

## **Task 5: Examine sympathetic innervation, tumor and non-tumor cell types expressing $\beta$ -AR, and collagen ordering in human breast tumors.**

(Months 24-30)

In our last report, we discussed our findings of the presence of tyrosine hydroxylase-positive (TH<sup>+</sup>) sympathetic nerve fibers within 4T1 tumors and their association with CD31<sup>+</sup> blood vessel endothelial cells. In the course of these experiments, we did not have time to investigate the relationship between  $\beta$ -AR expression, TH<sup>+</sup> noradrenergic nerve fiber, and collagen ordering in paraffin-embedded tumor biopsies from breast cancer patients. Others in the lab intend to conduct this work since I am leaving to return to medical school.

### **KEY RESEARCH ACCOMPLISHMENTS** (*\*denotes accomplishments from previous report*)

*\*We demonstrated that the impact of social isolation is of limited duration. This may be of particular significance when a tumor is slow-growing.*

*\*Using 4T1, an aggressive breast tumor model that does not express detectable  $\beta$ -AR, we demonstrated that NE elevates tumor growth but not metastasis, suggesting that tumor stromal cell components may facilitate tumor cell growth, even when the tumor is not able to directly respond to NE.*

*\*The mechanism(s) mediating the desipramine-induced increase in tumor growth is not increased VEGF and IL-6 production, key drivers of angiogenesis, as we originally hypothesized, suggesting alternative mechanisms may elicit primary tumor growth upon stressor exposure and activation of the sympathetic nervous system.*

- Selective  $\alpha$ 2-AR stimulation by dexmedetomidine increased breast tumor growth and metastasis.
- Neither NE, through desipramine treatment, nor  $\alpha$ 2-AR stimulation altered tumor angiogenesis.
- Tumor collagen microstructure is altered by elevated NE, suggesting a novel mechanism driven by changes in the tumor extracellular matrix that may contribute to tumor pathogenesis.

### **REPORTABLE OUTCOMES**

**Dissertation Defense:** Evidence for Sympathetic Nervous System Regulation of Breast Cancer Progression. June 22, 2012.

#### **Publications:**

**Szpunar MJ**, Burke KA, Brown EB, Madden KS. Chronically elevated norepinephrine and  $\alpha$ 2-AR stimulation promotes breast tumor progression through alterations in collagen structure. *In preparation.*

Madden KS, **Szpunar MJ**, Brown EB. Early impact of social isolation and breast tumor progression in mice. *Brain Behav Immun*. 2012. *Epub ahead of print*. PMID: 22610067.

**Oral Presentations:**

**Szpunar MJ**, Burke KA, Byun DK, Liverpool KM, Brown EB, Madden KS. Evidence for sympathetic nervous system modulation of mammary tumor pathogenesis via tumor collagen. Gordon Research Seminar: Mammary Gland Biology. Barga, Italy. June 9-10, 2012.

**Szpunar MJ**, Burke KA, Byun DK, Liverpool KM, Brown EB, Madden KS. Sympathetic nervous system activation and function in a beta-adrenergic receptor negative breast cancer model. Medical Scientist Research Symposium – University of Rochester, January 13, 2012.

**Poster Presentations:**

**Szpunar MJ**, Burke KA, Byun DK, Liverpool KM, Brown EB, Madden KS. Evidence for sympathetic nervous system modulation of mammary tumor pathogenesis via tumor collagen. Gordon Research Conference: Mammary Gland Biology. Barga, Italy. June 10-15, 2012.

Madden KS, **Szpunar MJ**, Burke KA, Byun DK, Liverpool KM, Brown EB. Evidence for sympathetic nervous system modulation of mammary tumor pathogenesis via tumor collagen. Psychoneuroimmunology Research Society Meeting. San Diego, CA. June 6-9, 2012.

**Szpunar MJ**, Madden KS, Liverpool KM, Brown EB. Sympathetic nervous system innervation and function in breast cancer models. American Association for Cancer Research: Tumor Microenvironment Complexity. Orlando, FL. November 3-6, 2011.

## CONCLUSION

Breast cancer is the most common cancer in women in the United States, and patients experience chronic emotional stress with cancer diagnosis and successive treatment. The aim of the work described here aimed to define biological mechanisms governing how stress and sympathetic nervous system activation affect breast tumor progression. We hypothesized that stress-induced release of NE augments breast tumor growth through stimulation of  $\alpha$ - or  $\beta$ -AR. We initially focused on SNS activation and  $\beta$ -AR stimulation since a role for  $\beta$ -AR signaling has been demonstrated in stress- and NE-induced alterations in tumor progression and in vitro responses of a variety of cancer types. We discovered a potentially clinically significant role for  $\alpha$ 2-AR in promoting breast tumor growth and metastasis. Furthermore, these results suggest that elevated NE and  $\alpha$ 2-AR stimulation in the 4T1 mammary tumor model elicit extracellular matrix changes, and propose a unique matrix-based mechanism for sympathetic activation-induced alterations in tumor pathogenesis. These changes reveal that NE stimulation of the tumor microenvironment is complex. Because NE can act as an agonist for multiple receptors, it can simultaneously cause different effects in different cell types within a tumor that contribute to tumor progression. Nevertheless, the overall result is a protumorigenic signal that augments tumor progression in the 4T1 tumor model, and we believe this result will be true in other breast tumor models, and furthermore, in at least some patient breast tumors.

Breast cancer is not one disease but a heterogeneous group of diseases, and personalized approaches are essential for more effective patient treatment. Our results imply that AR signaling and functional outcome vary considerably between breast cancers. Importantly, we have provided evidence that SNS activation and NE may influence breast tumor progression through modulation of the tumor extracellular matrix. *Therapeutics designed to block the biological mechanisms underlying stress-induced tumor growth and/or metastasis may prove of beneficial for breast cancer patients.*

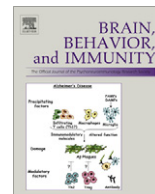
## REFERENCES

1. Andersen BL, Yang H, Farrar W, et al. Psychological intervention improves survival for breast cancer patients. *Cancer*. 2008;113(12): 3450-3458.
2. Thaker PH, Han LY, Kamat AA, et al. (2006) Chronic stress promotes tumor growth and angiogenesis in a mouse model of ovarian carcinoma. *Nat Med*. 2006;12(8): 939-44.
3. Sloan EK, Priceman SJ, Cox BF, et al. The sympathetic nervous system induces a metastatic switch in primary breast cancer. *Cancer Res*. 2010;70(18): 7042-52.
4. Sica A, Allavena P, Mantovani A. Cancer related inflammation: the macrophage connection. *Cancer Lett*. 2008;267(2): 204-15.
5. Pollard JW. Tumour-educated macrophages promote tumour progression and metastasis. *Nat Rev Cancer*. 2004;4(1): 71-8.
6. Vandewalle B, Revillion F, Lefebvre J. Functional beta-adrenergic receptors in breast cancer cells. *J Cancer Res Clin Oncol*. 1990;116(3): 303-6.
7. Slotkin TA, Zhang J, Dancel R, et al. Beta-adrenoceptor signaling and its control of cell replication in MDA-MB231 human breast cancer cell. *Breast Cancer Res Treat*. 2000;60(2): 153-66.
8. Madden KS, Szpunar MJ, Brown EB.  $\beta$ -Adrenergic receptors ( $\beta$ -AR) regulate VEGF and IL-6 production by divergent pathways in high  $\beta$ -AR-expressing breast cancer cell lines. *Breast Cancer Res Treat*. 2011;130(3):747-58.
9. Powe DG, Voss MJ, Habashy HO, et al. Alpha- and beta-adrenergic receptor (AR) protein expression is associated with poor clinical outcome in breast cancer: an immunohistochemical study. *Breast Cancer Res Treat*. 2011;130(2): 457-63.
10. Vázquez SM, Mladovan AG, Pérez C, et al. Human breast cell lines exhibit functional alpha2-adrenoceptors. *Cancer Chemother Pharmacol*. 2006;58(1): 50-61.
11. Nance DM, Sanders VM. Autonomic innervation and regulation of the immune system (1987-2007). *Brain Behav Immun*. 2007;21(6): 736-45.
12. Hammon HM, Bruckmaier RM, Honegger UE, Blum JW. Distribution and density of alpha- and beta-adrenergic receptor binding sites in the bovine mammary gland. *J Dairy Res*. 1994;61(1): 47-57.
13. Bruzzzone A, Pérez Piñero C, Rojas P, et al.  $\alpha(2)$ -Adrenoceptors enhance cell proliferation and mammary tumor growth acting through both the stroma and the tumor cells. *Curr Cancer Drug Targets*. 2011;11(6): 763-74.
14. Bockhorn M, Jain RK, Munn LL. Active versus passive mechanisms in metastasis: do cancer cells crawl into vessels, or are they pushed? *Lancet Oncol*. 2007;8(5): 444-8.
15. Brown EB, McKee T, diTomaso E, Pluen A, Seed B, Boucher Y, Jain RK. Dynamic imaging of collagen and its modulation in tumors in vivo using second-harmonic generation. *Nat Med*. 2003;9(6): 796-800.
16. Mertz J, Moreaux L. Second-harmonic generation by focused excitation of inhomogeneously distributed scatterers. *Opt Commun*. 2001;196: 325-30.
17. Sidani M, Wyckoff J, Xue C, et al. Probing the microenvironment of mammary tumors using multiphoton microscopy. *J Mammary Gland Biol Neoplasia*. 2006;11(2): 151-63.
18. Wang W, Wyckoff JB, Centonze F, et al. Single cell behavior in metastatic primary mammary tumors correlated with gene expression patterns revealed by molecular profiling. *Cancer Res*. 2002;62(21): 6278-88.

19. Condeelis J, Segall JE. Intravital imaging of cell movement in tumours. *Nat Rev Cancer*. 2003;3(12): 921-30.
20. Provenzano PP, Eliceiri KW, Campbell JM, et al. Collagen reorganization at the tumor-stromal interface facilitates local invasion. *BMC Med*. 2006;4(1): 38.
21. Conklin MW, Eickhoff JC, Riching KM, et al. Aligned collagen is a prognostic signature for survival in human breast carcinoma. *Am J Pathol*. 2011;178(3): 1221-32.

Contents lists available at [SciVerse ScienceDirect](http://www.sciencedirect.com)

## Brain, Behavior, and Immunity

journal homepage: [www.elsevier.com/locate/ybrbi](http://www.elsevier.com/locate/ybrbi)

## Early impact of social isolation and breast tumor progression in mice

Kelley S. Madden<sup>a,\*</sup>, Mercedes J. Szpunar<sup>b</sup>, Edward B. Brown<sup>a</sup><sup>a</sup> Department of Biomedical Engineering, University of Rochester School of Medicine and Dentistry, Rochester, NY, USA<sup>b</sup> Department of Pathology, University of Rochester School of Medicine and Dentistry, Rochester, NY, USA

## ARTICLE INFO

Article history:  
Available online xxxxxKeywords:  
Social isolation  
Psychosocial stressor  
Breast cancer  
Norepinephrine  
Macrophages  
SCID mice

## ABSTRACT

Evidence from cancer patients and animal models of cancer indicates that exposure to psychosocial stress can promote tumor growth and metastasis, but the pathways underlying stress-induced cancer pathogenesis are not fully understood. Social isolation has been shown to promote tumor progression. We examined the impact of social isolation on breast cancer pathogenesis in adult female severe combined immunodeficiency (SCID) mice using the human breast cancer cell line, MDA-MB-231, a high  $\beta$ -adrenergic receptor (AR) expressing line. When group-adapted mice were transferred into single housing (social isolation) one week prior to MB-231 tumor cell injection into a mammary fat pad (orthotopic), no alterations in tumor growth or metastasis were detected compared to group-housed mice. When social isolation was delayed until tumors were palpable, tumor growth was transiently increased in singly-housed mice. To determine if sympathetic nervous system activation was associated with increased tumor growth, spleen and tumor norepinephrine (NE) was measured after social isolation, in conjunction with tumor-promoting macrophage populations. Three days after transfer to single housing, spleen weight was transiently increased in tumor-bearing and non-tumor-bearing mice in conjunction with reduced splenic NE concentration and elevated CD11b + Gr-1+ macrophages. At day 10 after social isolation, no changes in spleen CD11b+ populations or NE were detected in singly-housed mice. In the tumors, social isolation increased CD11b + Gr-1+, CD11b + Gr-1-, and F4/80+ macrophage populations, with no change in tumor NE. The results indicate that a psychological stressor, social isolation, elicits dynamic but transient effects on macrophage populations that may facilitate tumor growth. The transiency of the changes in peripheral NE suggest that homeostatic mechanisms may mitigate the impact of social isolation over time. Studies are underway to define the neuroendocrine mechanisms underlying the tumor-promoting effects of social isolation, and to determine the contributions of increased tumor macrophages to tumor pathogenesis.

© 2012 Elsevier Inc. All rights reserved.

## 1. Introduction

The emotional stress experienced by cancer patients can be associated with increased tumor progression (Antoni et al., 2006), but the biological pathways involved in stress-induced tumor progression are only beginning to be understood. In animal models of cancer, exposure to stressors potentiates tumor growth and metastasis in a variety of tumors (Hermes et al., 2009; Saul et al., 2005; Shakhar and Ben-Eliyahu, 1998; Sloan et al., 2010; Thaker et al., 2006; Williams et al., 2009) suggesting that therapies targeting stress biochemical pathways may be effective in reducing tumor progression. Here we examine the impact of social isolation of adult mice, an ethologically relevant

stressor, on breast tumor growth. Social isolation in rodents elicits anxiety and other fearful behaviors (Hermes et al., 2009; Williams et al., 2009). Furthermore, chronic social isolation as experienced by humans has been linked to cancer (Reynolds and Kaplan, 1990), and is a risk factor for cancer mortality and other diseases (Hawkey and Cacioppo, 2003).

The sympathetic nervous system (SNS) is a major stressor pathway characterized by release of the catecholamines norepinephrine (NE) and epinephrine (EPI) from sympathetic noradrenergic nerves and from the adrenal medulla. Several lines of evidence point to a role for the SNS in modulating tumor progression. Regional ablation of sympathetic nerves depleted NE and reduced tumor growth (Raju et al., 2007). Stress-induced increase in tumor growth and/or metastasis can be prevented by pre-treatment with a  $\beta$ -AR blocker prior to stressor exposure or mimicked using  $\beta$ -AR agonists *in vivo* (Shakhar and Ben-Eliyahu, 1998; Sloan et al., 2010; Thaker et al., 2006). Furthermore, using an ovarian cancer model, Thaker and colleagues showed that  $\beta$ -AR expression by the tumor cells was necessary for stressor-induced tumor growth (Thaker et al., 2006). It is interesting to note the variety of targets in stress- and

Abbreviations: IL-6, Interleukin 6; SNS, sympathetic nervous system; NE, norepinephrine; EPI, epinephrine;  $\beta$ -AR, beta-adrenergic receptors; VEGF, vascular endothelial growth factor.

\* Corresponding author. Address: Department of Biomedical Engineering, University of Rochester School of Medicine and Dentistry, RC Box 270168, Goergen Hall, Rochester, NY 14627, USA. Tel.: +1 585 273 5724; fax: +1 585 276 2254.

E-mail address: [Kelley\\_Madden@urmc.rochester.edu](mailto:Kelley_Madden@urmc.rochester.edu) (K.S. Madden).

or SNS-induced potentiation of tumor progression including cells of the immune system (for example, macrophages and natural killer cells) (Shakhar and Ben-Eliyahu, 1998; Sloan et al., 2010), angiogenesis (Thaker et al., 2006), and direct stimulation or inhibition of tumor proliferation (Slotkin et al., 2000). In addition to understanding the stress-induced neuroendocrine mediators/receptors that modulate tumor pathogenesis, it is also important to identify the target cells in order to predict the outcome of stress exposure and to develop therapies with minimal side effects.

The MDA-MB-231 cell line is a human mammary tumor adenocarcinoma representative of the more aggressive triple negative human breast cancer. MB-231 cells express high levels of  $\beta$ -AR, as detected by standard radioligand binding assay, but other breast cancer cell lines displayed a low level of  $\beta$ -AR expression and minimal responsiveness to NE *in vitro* (Madden et al., 2011). By contrast, NE stimulation of MB-231 cells inhibits VEGF production, and dramatically increases IL-6 production *in vitro*. With the view that MB-231 serves as a model of breast cancers expressing high levels of  $\beta$ -AR, we have begun testing the impact of stressor exposure on MB-231 tumor growth, using social isolation as an established model of a psychological stressor that can promote tumor progression, including spontaneous mammary tumor progression (Hermes et al., 2009; Thaker et al., 2006; Williams et al., 2009).

We report here that social isolation transiently increased tumor growth only when social isolation was initiated when tumors were palpable. These changes were associated with alterations in tumor macrophage populations early after social isolation and not associated with elevated tumor or peripheral NE concentration. The results demonstrate the complexity of the response of breast tumors to stressor exposure that needs to be better characterized before targeting stress hormones in the therapeutic treatment of breast cancer.

## 2. Materials and methods

### 2.1. Mice

Female severe combined immunodeficiency (SCID) (NOD.CB17-Prkdc<sup>scid</sup>/J) mice were purchased from The Jackson Laboratory, Bar Harbor, ME between 6 and 8 weeks of age, and were housed 5 per cage with food and water ad lib on a 12:12 light:dark cycle. SCID mice were provided acid water ad lib upon arrival. The mice were housed using microisolator technology to effect a biological barrier at the level of the individual cage. Upon initiation of the experiments, the antibiotic sulfamethoxazole and trimethoprim (Hi-Tech Pharmacol. Co., Amityville, NY) was included in the drinking water throughout the duration of the experiment. The antibiotic treatment was necessary in order to prevent the occasional pneumonia that developed in these immunodeficient mice. All experimental protocols were approved by the University of Rochester University Committee on Animal Resources.

### 2.2. Cell lines

MB-231 tumor cells (American Tissue Type Collection; Manassas, VA) were maintained in Dulbecco's Modified Essential Medium (DMEM) containing 4.5 g/L glucose, L-glutamine, penicillin/streptomycin and 10% fetal calf serum (FCS) (all from Gibco, Invitrogen Inc., Carlsbad, CA). MB-231 cells were employed experimentally within 3 months of acquiring and/or thawing, and were regularly tested for the absence of mycoplasma contamination.

### 2.3. Social isolation

SCID mice were allowed to adapt to group housing (5 per cage) for at least two weeks before being housed singly. Both group- and single-housed mice were housed in cages measuring 7.5"  $\times$  11"  $\times$  5".

### 2.4. Tumor implantation and measures

MB-231 ( $2\text{--}4 \times 10^6$  cells) was injected into a single mammary fat pad of NOD/SCID female mice in mice anesthetized with 90 mg/kg ketamine and 9 mg/kg xylazine. Mice were palpated weekly until tumors were detected. The shortest and longest diameters of each tumor were measured with calipers. Tumor volumes was calculated using the equation:  $0.5 \times \text{length} \times \text{width}^2$ .

### 2.5. Flow cytometry

Single suspensions from spleen or tumors were prepared by pressing tissue through a metal mesh into ice-cold PBS containing 10% fetal calf serum. Red blood cells were lysed using ammonium lysis buffer. After washing, the cells were counted and resuspended in phosphate buffered saline containing 1% bovine serum albumin and 0.25% sodium azide (flow wash). Macrophages were stained using three-color immunofluorescence. Cells ( $1.5 \times 10^6$ ) were incubated in 25  $\mu$ l FcBlock (anti-CD16, diluted 1:50; BD Biosciences, bdbiosciences.com) for 15 min at 4 °C. Rat anti-F4/80 (clone BM8; FITC-conjugated; Abcam Inc.; abcam.com), rat anti-CD11b (clone M1/70; Alexafluor 647-conjugated, BD Biosciences) and rat anti-Gr-1 (anti-Ly-6G and Ly-6C; clone RB6-8C5; PE-conjugated; BD Biosciences) were diluted 1:50 in flow wash. Antibodies (100  $\mu$ l) were incubated 30 min at 4 °C. Cells incubated in flow wash only served as autofluorescent controls. Cells were washed two times in flow wash, fixed in 0.5 ml PBS containing 1% paraformaldehyde, and stored in the dark at 4 °C for no longer than 2 weeks before analysis. Fluorescence was analyzed in the University of Rochester Flow Cytometry Core on a BD LSR II 18-Color flow cytometer. Forward scatter and side scatter gating was used to eliminate non-lymphoid cells from the analysis. Analysis gates were set based on the autofluorescent controls.

### 2.6. Cytokine and norepinephrine determination

For cytokines, tumor homogenates at a concentration of 4% w/v were prepared in RIPA buffer containing protease inhibitors (HALT Protease Inhibitor Cocktail, Thermoscientific; Thermofisher.com). To measure NE, tumors were homogenized at a concentration of 1% w/v in 1 N HCl. Protein in homogenates was measured colorimetrically using a Pierce BCA Protein Assay kit (Thermoscientific). NE and tumor cytokines in the homogenates were measured by ELISA according to the manufacturer's instructions. A NE ELISA kit was purchased from Rocky Mountain Diagnostics. Mouse- and human-specific VEGF and IL-6 Quantikine kits (R and D Systems, Minneapolis, MN) are highly species specific with little or no cross-reactivity detected with the corresponding analyte from other species. As reported by the manufacturer and confirmed in our laboratory, the only (minimal) cross-reactivity detected is 0.2% cross-reactivity of human VEGF in the mouse VEGF ELISA. Serial dilutions of the tumor homogenates were tested to determine the optimal homogenate dilution for each analyte. Absorption was measured at 450 nm using a multiwell plate reader (Synergy HT, Biotek Instruments Inc., Winooski, VT). Curve fitting and sample concentration calculations were conducted with Gen5 software (Biotek). Results were normalized based on protein concentration or tissue wet weight.

### 2.7. Statistical analysis

Statistically significant differences between groups were determined using GraphPad Prism software. For all analyses,  $p < 0.05$  is considered statistically significant. When comparing two groups, *F*-test for equality of variance was used to determine if the variance differed significantly. If variance between the two groups was

equal, Student's *t*-test was used. For non-equal variance, non-parametric Mann–Whitney was used as indicated. To compare more than two groups, a significant main effect by one-way ANOVA was followed by post hoc Newman–Keuls analysis. Tumor volume over time was analyzed using a two-way repeated measures ANOVA, and significant main effects or interactions were analyzed using Bonferroni's post hoc analysis.

### 3. Results

#### 3.1. Social isolation prior to MB-231 tumor cell injection

We have investigated the impact of stressor exposure in the form of social isolation on orthotopic growth of the human breast tumor cell line, MB-231, in SCID female mice. Mice were separated into single housing one week prior to MB-231 tumor cell injection ( $2 \times 10^6$  cells) into the mammary fat pad. Fig. 1 represents results from three experimental repetitions in which tumor growth was measured over time. In these experimental repetitions, tumor NE, human and mouse VEGF and IL-6 were not consistently altered at the time of sacrifice (day 83 post-MB-231 injection in Fig. 1; data not shown). No difference in lung metastases (the only site of metastasis from the primary MB-231 tumor) was observed between the two groups (data not shown). We postulated that the inability to produce replicable changes in tumor growth was due to the fact that MB-231 is a slow growing tumor *in vivo*, allowing mice to adapt to social isolation. If true, we predicted that social isolation would have a greater impact if transfer to single housing took place closer to the exponential phase of tumor growth.

#### 3.2. Social isolation after MB-231 injection

To test this possibility, SCID mice were injected orthotopically with MB-231 ( $4 \times 10^6$  cells) and tumor growth was monitored over time. One-half of the mice were singly housed when tumors were palpable in all mice (in this experiment, day 14 post-tumor injection; average tumor volume =  $\sim 25$  mm<sup>3</sup>). The other mice remained in their home cages, and tumor growth in all mice was measured over time. MB-231 tumor growth was greater in singly-housed compared to group-housed mice when tumor volume was analyzed through day 28 post-separation (Fig. 2A; repeated measures ANOVA, main effect of housing,  $p < 0.03$  with no interaction by time,  $p = 0.5$ ). By day 34 post-separation, the effect of social isolation had dissipated somewhat. When this time point was included in the analysis, the main effect was no longer significant

( $p = 0.07$ ) with no interaction by day post-separation ( $p = 0.6$ ). Mice were sacrificed at this time point (day 34 post-separation). Tumor weight did not differ between groups (data not shown). Interestingly, a trend towards reduced tumor NE in the singly-housed group was noted (Fig. 2B, Mann–Whitney,  $p = 0.1$ ). Tumor human VEGF concentration did not differ between groups (data not shown), but a trend towards increased human IL-6 was noted in tumors from singly-housed mice (Fig. 2C; Mann–Whitney,  $p = 0.1$ ). Mouse IL-6 did not differ between groups (data not shown). No difference in lung metastases was observed between the two groups (data not shown). These results demonstrate that social isolation facilitated tumor progression, but the duration of the effect on tumor growth was limited.

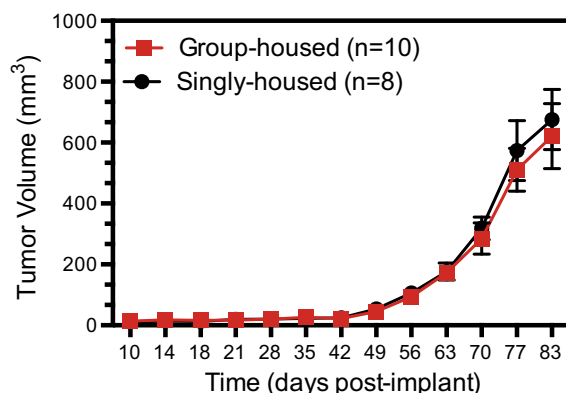


**Fig. 1.** MB-231 tumor growth is not altered by social isolation prior to tumor cell injection. SCID female mice were singly housed seven days prior to orthotopic injection of MB-231 cells. Tumor diameter was measured with calipers on the days indicated. Tumor volume is expressed as mean  $\pm$  SEM,  $n = 8$ –10 mice per group.

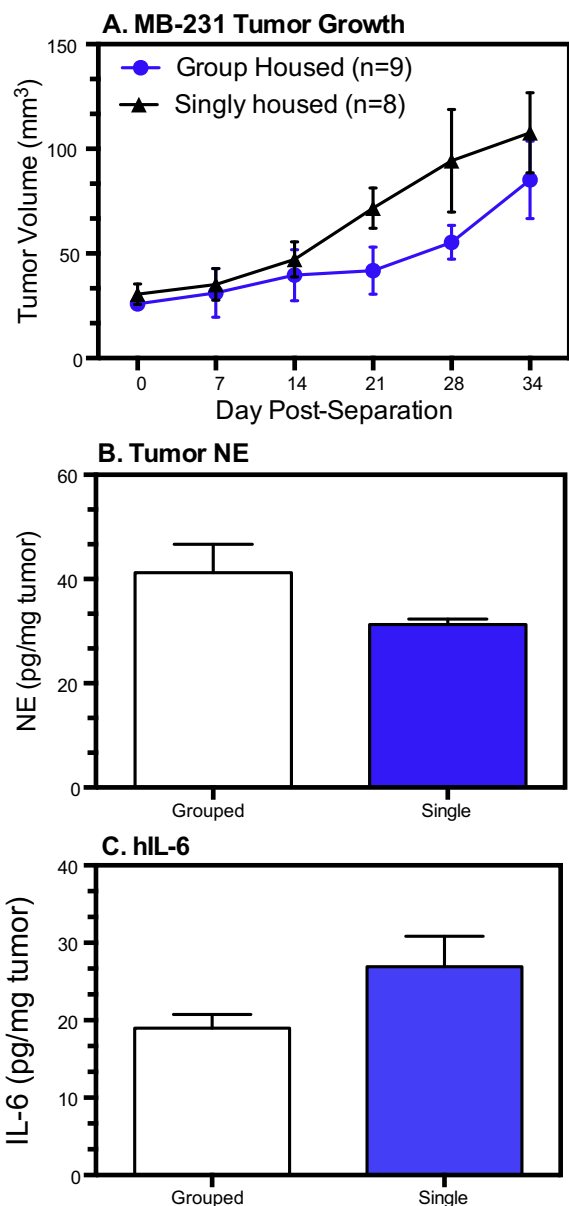


**Fig. 2.** MB-231 tumor growth is transiently increased by social isolation after tumor injection. SCID female were injected with MB-231 cells, and when all mice had palpable tumors, half of the mice were transferred from group to single housing. (A) Tumor volume over time. NE (B) and human IL-6 (C) were measured by ELISA in tumors harvested at day 34 post separation. Results are expressed as mean  $\pm$  SEM,  $n = 8$ –9 mice per group. See text for statistical analysis of tumor growth. For tumor NE and human IL-6, no significant effects based on the non-parametric Mann–Whitney test,  $p = 0.1$ .

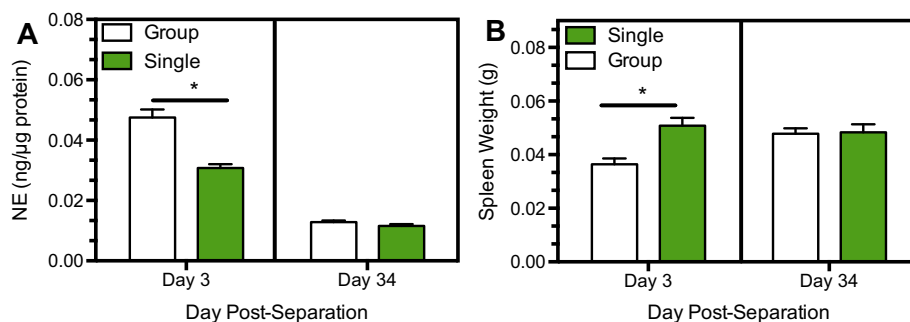


**Fig. 3.** Social isolation reciprocally alters spleen NE (A) and spleen weight (B) early after social isolation. A subset of mice described in Fig. 2 was sacrificed at day 3 post-separation. Results are expressed as mean  $\pm$  SEM,  $n = 5$  mice per group. Asterisk indicates different versus group-housed at the corresponding time point by Newman-Keuls post hoc analysis.

In this same experiment, a subset of mice was sacrificed day 3 after social isolation to determine if sympathetic activation occurred early after social isolation. At this time point, the tumors ( $\leq 10$  mg in weight) were too small to measure NE; therefore the spleen was used as a highly-innervated surrogate organ to compare NE concentration after social isolation. Day 3 post-separation, splenic NE concentration was significantly reduced in the singly-housed mice (Fig. 3A; ANOVA, housing  $\times$  day interaction,  $p < 0.001$ ). The decrease in NE concentration was associated with increased spleen weight (Fig. 3B; ANOVA, housing  $\times$  day interaction,  $p = 0.02$ ), suggesting that the increase in spleen mass reduced NE concentration in the singly housed mice. By day 34 post separation, neither NE concentration nor spleen weight was altered in singly-housed compared to group-housed mice, but compared to day 3, splenic NE concentration was significantly reduced in both groups in conjunction with increased spleen mass (ANOVA, main effect of day,  $p < 0.001$ ).

### 3.3. Effects of social isolation on increased spleen mass are not dependent on tumor

In the next experiment, to determine if the early effect of social isolation on spleen mass was dependent on the presence of growing tumors, non-tumor bearing SCID female mice were socially isolated. In addition, flow cytometry was used to determine if

macrophage populations were altered after social isolation, as reported for other social stressors (Engler et al., 2004). Social isolation increased spleen weight at this time point in association with decreased spleen NE concentration (Fig. 4A and B), similar to the effects at d3 in tumor-bearing mice. The percentage of splenic macrophages expressing F4/80+ and CD11b+ Gr-1-cells was not significantly altered (Fig. 4C and E), but the percentage of CD11b+ macrophages that co-express Gr-1+ were significantly increased in socially isolated mice. These cells are myeloid derived suppressor cells that have potent immunosuppressive capabilities (Gabrilovich and Nagaraj, 2009). These results demonstrate that the early effect of social isolation in the spleen is independent of tumor growth, and that specific splenic macrophage populations are sensitive to neurohormonal changes elicited by social isolation. Since these macrophage populations are important regulators of tumor progression, we tested if macrophage populations are altered in spleens and tumors of socially isolated mice.

### 3.4. Social isolation alters spleen and tumor macrophage populations

The next experiment examined alterations in spleen and tumor NE concentration and macrophage populations 10 days after social isolation in mice bearing tumors. Social isolation was initiated when average tumor volume was  $\sim 50$  mm<sup>3</sup>. Social isolation did not alter spleen or tumor weight or NE concentration 10 days after

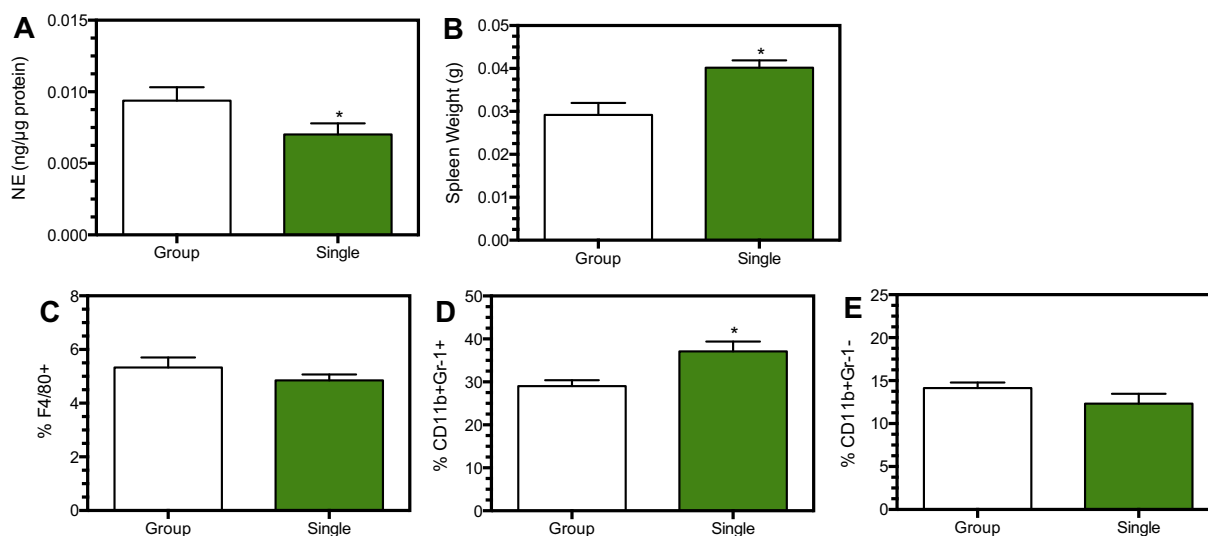


**Fig. 4.** Early effects of social isolation on spleen NE and spleen weight is independent of tumor growth. Three days after transfer to single housing, SCID female mice were sacrificed and spleen NE (A), weight (B), and macrophage populations (C–E) were determined. Asterisk indicates significant difference by Student's *t*-test,  $p < 0.05$ . Results are expressed as mean  $\pm$  SEM,  $n = 5$  mice per group.

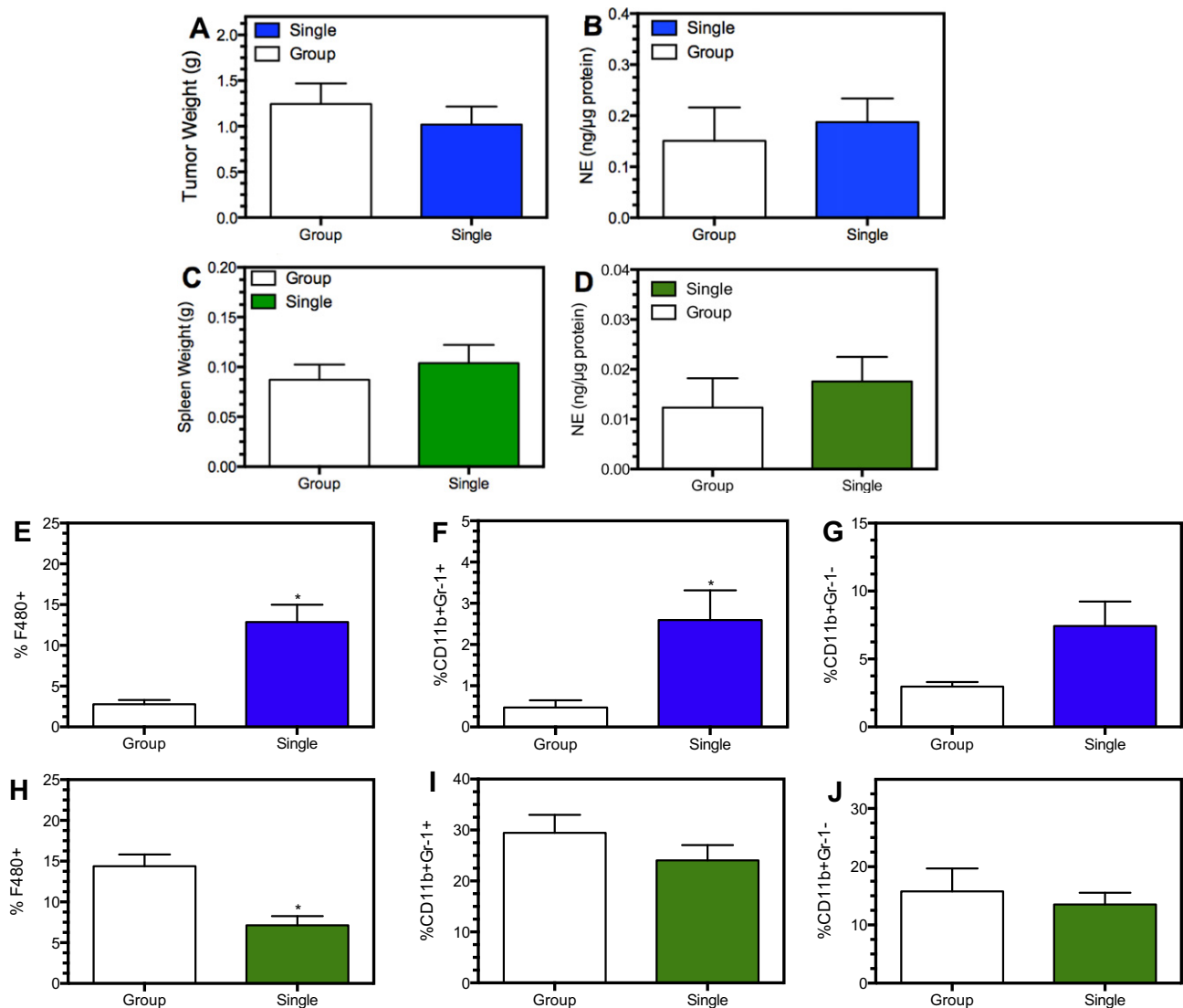


**Fig. 5.** Social isolation alters tumor and spleen macrophage populations. SCID female mice were injected with MB-231 in the mammary fat pad. When tumors were palpable, one-half the mice were transferred from group-housing to single housing. After 10 days, mice were sacrificed and tumor (A and B) and spleen (C and D) weight and NE concentration were determined, and macrophage populations were analyzed by flow cytometry in tumors (E–G) and spleens (H–J). Asterisk indicates significance based on the non-parametric Mann–Whitney test (A and B) or by student's *t*-test (D),  $p < 0.05$ . In (C),  $p = 0.067$ . The results are expressed as mean  $\pm$  SEM of 9–10 mice per group.

social isolation (Fig. 5A–D). However, macrophage populations were increased in tumors from socially isolated mice with significant increases in the percentage of F4/80+ (Fig. 5E) and CD11b + Gr-1+ populations (Fig. 5F) and a trend toward an increase in the CD11b + Gr-1- population (Fig. 5G). In the spleen, the percentage of F480+ macrophages was reduced (Fig. 5H) with no significant changes in either CD11b+ population (Fig. 5I and J). These results demonstrate distinct changes in tumor and spleen macrophage populations with social isolation.

#### 4. Discussion

Social isolation is a well-characterized social stressor that has several advantages to more standard laboratory-type stressors. It is a milder form of stress compared to other forms of stressor exposure. For example, in our hands singly-housed mice do not lose weight (data not shown) nor display elevated tissue NE concentration, in contrast to the weight loss (Sloan et al., 2010) and increased tissue NE concentration (Thaker et al., 2006) reported with daily restraint stress. Yet animals exposed to social isolation

mimic behavioral anxiety and increased vigilance associated with social isolation observed in humans (Hermes et al., 2009; Williams et al., 2009). Here, we demonstrated that social isolation transiently increased MB-231 tumor growth, but only when social isolation was initiated when tumor growth was near exponential phase. No consistent effects of tumor growth or metastasis were observed when social isolation occurred prior to MB-231 injection, suggesting a temporal dependence in the context of a mild stressor. Indeed, early and transient changes in spleen NE concentration and macrophage populations, independent of whether or not the animals were tumor-bearing, were observed. Furthermore, increases in tumor macrophage populations took place before any indications of altered tumor growth. The changes in macrophage populations in the tumors were not associated with altered tumor NE. These results suggest that social isolation can have an impact on tumor progression, but the impact is transient and may not be associated with dramatic changes in tumor growth and metastasis.

The changes in macrophage populations in tumor and spleen indicate that social isolation facilitates leukocyte recruitment – a process described with another social stressor, social disruption

(Engler et al., 2004). Repeated social disruption increased spleen weight in concert with loss of CD11b<sup>+</sup> myeloid cells from the bone marrow and an increase in CD11b<sup>+</sup> cells in the spleen. Furthermore, the increase in spleen weight elicited by social disruption was mediated through  $\beta$ -AR stimulation, as it was prevented by propranolol pretreatment to block  $\beta$ -AR (Wohleb et al., 2011). The increase in the CD11b<sup>+</sup>Gr-1<sup>+</sup> population in spleen from non-tumor bearing, singly-housed mice shown here (Fig. 4), suggests that this process also occurs with social isolation. A similar stress-induced increase in tumor macrophages has been described by Sloan and colleagues, who demonstrated elevated F4/80<sup>+</sup> tumor macrophages and a trend toward increased myeloid derived suppressor cells with restraint stress; this effect was blocked by propranolol treatment (Sloan et al., 2010). Restraint stress did not facilitate primary tumor growth, but increased tumor angiogenesis and dramatically elevated metastasis (Sloan et al., 2010). In our hands, tumor associated macrophage populations expressing F4/80 and CD11b were increased with social isolation. The spleen is an important source of tumor associated macrophages and tumor associated neutrophils (Cortez-Retamozo et al., 2012). The social isolation-induced decrease in the splenic F4/80<sup>+</sup> population in conjunction with an increase in this population in tumors suggests that the spleen may contribute to the increased F4/80<sup>+</sup> tumor associated macrophages in socially isolated mice. It is likely that both the spleen and bone marrow may be targets of stress hormones that promote the migration of these macrophage populations into the tumor. Both tumor associated macrophages and myeloid derived suppressor cell populations are associated with tumor progression (Gabrilovich and Nagaraj, 2009), but we have yet to establish that the increased tumor macrophages lead to the increased tumor growth in the singly-housed mice.

Social isolation has been characterized as a stressor based on behavior (it elicits anxiety behaviors in female mice) (Palanza et al., 2001), but is less well characterized in terms of hypothalamic pituitary axis or sympathetic nervous system activation. Long-term social isolation increased development of spontaneous mammary tumors and metastasis, but these rats were socially isolated from puberty (Hermes et al., 2009), making it difficult to directly compare to the social isolation procedure here, which was begun when the mice had reached adulthood. Nonetheless, social isolation led to reduced baseline levels of plasma corticosterone at the nadir of the diurnal rhythm in social isolated rats, but an elevated and prolonged corticosterone response to a stressor (Hermes et al., 2009; Williams et al., 2009). Similarly, a 21-day period of single housing did not alter baseline plasma catecholamines, but upon exposure to an acute stressor, plasma catecholamines in socially isolated rats were significantly elevated versus group-housed (Dronjak et al., 2004). Therefore, the social isolation model will be particularly useful for examining the impact of an acute stressor in animals exposed to long-term social isolation. The results presented here suggest that social isolation alone may elicit alterations that have a transient impact. Future plans include using social isolation to understand the biological consequences of multiple stressors on tumor pathogenesis, a more likely scenario in the context of a diagnosis of breast cancer.

The effects of social isolation were not associated with increased NE concentrations in spleen or in tumor, as might be expected if social isolation activated the SNS. However, there are a few caveats in interpreting tissue NE measures. First, NE concentration in the spleen appeared to fluctuate with changes in spleen mass. One way to interpret this finding is that sympathetic nerve fibers within the spleen do not respond rapidly to a rapid expansion in tissue volume, such as the increase in spleen weight with social isolation or even in a growing tumor. We can detect sympathetic nerve fibers in MB-231 tumors independent of tumor size, however the impact of the expanding tumor architecture on NE

concentration has not been systematically examined. Furthermore, measuring only tissue NE may not be an appropriate measure of SNS activation, especially under conditions of a relatively mild stressor such as social isolation where homeostatic mechanisms serve to maintain a constant tissue NE baseline (Eisenhofer et al., 2004). Therefore, we have begun to assess normetanephrine, a product of NE metabolism by catechol-O-methyltransferase, as a potential additional measure of sympathetic activation and re-leased NE. These experiments will help define the role of SNS activation and  $\beta$ -AR stimulation in the context of social isolation.

The results presented here demonstrate an early, but transient effect of a psychological stressor, social isolation, in both tumor-bearing and normal female SCID mice. The results imply that exposures to relatively mild stressors may promote tumor progression, depending on the timing relative to tumor growth, but also suggest the possibility that homeostatic mechanisms can mitigate the impact of social isolation. This is a potential area of investigation in terms of identifying pathways that help minimize the impact of chronic stress experienced in breast cancer patients. It is critical to understand how mild stressors interact to develop into a more severe stressor and to develop therapies that work in concert with standard breast cancer therapies to inhibit tumor progression.

### Grant support

This work was supported by Department of Defense IDEA Award (W81XWH-10-01-008) and National Institutes of Health (1 R21 CA152777-01) to KSM, Department of Defense Era of Hope Scholar Research Award (W81XWH-09-1-0405), National Institutes of Health Director's New Innovator Award (1 DP2 OD006501-01), and Pew Scholar in the Biomedical Sciences Award to EBB, and Department of Defense Predoctoral Training Award (W81XWH-10-1-0058) and predoctoral grant TL1 RR024135 from the National Center for Research Resources, a component of the NIH, and the NIH Roadmap for Medical Research to MJS. MJS is a trainee in the Medical Scientist Training Program funded by NIH T32 GM07356. The content is solely the responsibility of the authors and does not necessarily represent the official views of the National Institute of General Medical Sciences or NIH.

### Acknowledgments

We thank Khawar Liverpool, Dan Byun, Tracy Bubel, Giuseppe Arcuri, and Taylor Wolfgang for their excellent technical assistance.

### References

- Antoni, M.H., Lutgendorf, S.K., Cole, S.W., Dhabhar, F.S., Sephton, S.E., McDonald, P.G., Stefanek, M., Sood, A.K., 2006. The influence of bio-behavioural factors on tumour biology: pathways and mechanisms. *Nat. Rev. Cancer* 6, 240–248.
- Cortez-Retamozo, V., Etzrodt, M., Newton, A., Rauch, P.J., Chudnovskiy, A., Berger, C., Ryan, R.J., Iwamoto, Y., Marinelli, B., Gorbato, R., Forghani, R., Novobrantseva, T.I., Kotliansky, V., Figueiredo, J.L., Chen, J.W., Anderson, D.G., Nahrendorf, M., Swirski, F.K., Weissleder, R., Pittet, M.J., 2012. Origins of tumor-associated macrophages and neutrophils. *Proc. Natl. Acad. Sci. USA*.
- Dronjak, S., Gavrilovic, L., Filipovic, D., Radojic, M.B., 2004. Immobilization and cold stress affect sympatho-adrenomedullary system and pituitary-adrenocortical axis of rats exposed to long-term isolation and crowding. *Physiol. Behav.* 81, 409–415.
- Eisenhofer, G., Kopin, I.J., Goldstein, D.S., 2004. Catecholamine metabolism: a contemporary view with implications for physiology and medicine. *Pharmacol. Rev.* 56, 331–349.
- Engler, H., Bailey, M.T., Engler, A., Sheridan, J.F., 2004. Effects of repeated social stress on leukocyte distribution in bone marrow, peripheral blood and spleen. *J. Neuroimmunol.* 148, 106–115.
- Gabrilovich, D.I., Nagaraj, S., 2009. Myeloid-derived suppressor cells as regulators of the immune system. *Nat. Rev. Immunol.* 9, 162–174.
- Hawkey, L.C., Cacioppo, J.T., 2003. Loneliness and pathways to disease. *Brain Behav. Immun.* 17 (Suppl. 1), S98–S105.
- Hermes, G.L., Delgado, B., Tretiakova, M., Cavigelli, S.A., Krausz, T., Conzen, S.D., McClintock, M.K., 2009. Social isolation dysregulates endocrine and behavioral

- stress while increasing malignant burden of spontaneous mammary tumors. *Proc. Natl. Acad. Sci. USA* 106, 22393–22398.
- Madden, K.S., Szpunar, M.J., Brown, E.B., 2011. Beta-Adrenergic receptors (beta-AR) regulate VEGF and IL-6 production by divergent pathways in high beta-AR-expressing breast cancer cell lines. *Breast Cancer Res. Treat.* 130, 747–758.
- Palanza, P., Gioiosa, L., Parmigiani, S., 2001. Social stress in mice: gender differences and effects of estrous cycle and social dominance. *Physiol. Behav.* 73, 411–420.
- Raju, B., Haug, S.R., Ibrahim, S.O., Heyeraas, K.J., 2007. Sympathectomy decreases size and invasiveness of tongue cancer in rats. *Neuroscience* 149, 715–725.
- Reynolds, P., Kaplan, G.A., 1990. Social connections and risk for cancer: prospective evidence from the Alameda County Study. *Behav. Med.* 16, 101–110.
- Saul, A.N., Oberyzy, T.M., Daugherty, C., Kusewitt, D., Jones, S., Jewell, S., Malarkey, W.B., Lehman, A., Lemeshow, S., Dhabhar, F.S., 2005. Chronic stress and susceptibility to skin cancer. *J. Natl. Cancer Inst.* 97, 1760–1767.
- Shakhar, G., Ben-Eliyahu, S., 1998. In vivo b-adrenergic stimulation suppresses natural killer activity and compromises resistance to tumor metastasis in rats. *J. Immunol.* 160, 3251–3258.
- Sloan, E.K., Priceman, S.J., Cox, B.F., Yu, S., Pimentel, M.A., Tangkanangnukul, V., Arevalo, J.M., Morizono, K., Karanikolas, B.D., Wu, L., Sood, A.K., Cole, S.W., 2010. The sympathetic nervous system induces a metastatic switch in primary breast cancer. *Cancer Res.* 70, 7042–7052.
- Slotkin, T.A., Zhang, J., Dancel, R., Garcia, S.J., Willis, C., Seidler, F.J., 2000. Beta-adrenoceptor signaling and its control of cell replication in MDA-MB-231 human breast cancer cells. *Breast Cancer Res. Treat.* 60, 153–166.
- Thaker, P.H., Han, L.Y., Kamat, A.A., Arevalo, J.M., Takahashi, R., Lu, C., Jennings, N.B., Armaiz-Pena, G., Bankson, J.A., Ravoori, M., Merritt, W.M., Lin, Y.G., Mangala, L.S., Kim, T.J., Coleman, R.L., Landen, C.N., Li, Y., Felix, E., Sanguino, A.M., Newman, R.A., Lloyd, M., Gershenson, D.M., Kundra, V., Lopez-Berestein, G., Lutgendorf, S.K., Cole, S.W., Sood, A.K., 2006. Chronic stress promotes tumor growth and angiogenesis in a mouse model of ovarian carcinoma. *Nat. Med.* 12, 939–944.
- Williams, J.B., Pang, D., Delgado, B., Kocherginsky, M., Tretiakova, M., Krausz, T., Pan, D., He, J., McClintock, M.K., Conzen, S.D., 2009. A model of gene-environment interaction reveals altered mammary gland gene expression and increased tumor growth following social isolation. *Cancer Prev. Res.* 2, 850–861.
- Wohleb, E.S., Hanke, M.L., Corona, A.W., Powell, N.D., Stiner, L.M., Bailey, M.T., Nelson, R.J., Godbout, J.P., Sheridan, J.F., 2011. Beta-adrenergic receptor antagonism prevents anxiety-like behavior and microglial reactivity induced by repeated social defeat. *J. Neurosci.* 31, 6277–6288.